

Coherent Soft X-Ray Diffraction Imaging of Skyrmion Crystal in a Chiral Magnet FeGe

Coherent resonant soft X-ray diffraction was used to visualize the magnetic textures in a thin plate of the cubic B20 compound FeGe. Small-angle magnetic scattering patterns were successfully measured from a helical magnetic structure and skyrmion lattice. We first performed the lens-less imaging of an ordered magnetic texture with in-situ controlled temperature and magnetic field using an iterative phase retrieval approach. The method can be used with both circularly and linearly polarized soft X-ray beams, and does not require any focusing X-ray optics to perform magnetic imaging with a resolution of a few tens of nanometers.

Lens-less imaging with coherent X-rays has been successfully performed in various studies in the fields of nanotechnology, biology, and condensed matter physics [1]. The method is extremely useful for the structural examination of non-crystalline specimens, and can be used to determine the exact positions of individual scattering objects and to map defects in periodically ordered structures. One of the promising applications of coherent soft X-rays is the imaging of the local magnetization of magnetic specimens. In the soft X-ray regime, by exciting electrons from the 2p state to the 3d state of transition-metal atoms, it is possible to study the magnetic ordering in wide-angle diffraction [2] or small-angle scattering geometry [3-4]. Dichroic resonant soft X-ray scattering can be successfully combined with coherent diffraction approaches such as iterative phase retrieval [5] and Fourier transform holography-based methods [6].

In this study, we employed a phase retrieval algorithm to reconstruct lens-less images of the magnetic textures from the coherent small-angle resonant soft X-ray scattering (RSXS) patterns measured from the magnetically ordered compound FeGe [7]. Helical magnetic ordering appears in FeGe at zero field near room tem-

perature ($T_c = 280$ K) due to the interplay between the exchange interaction, Dzyaloshinskii–Moriya interaction, and anisotropy. By applying a moderate magnetic field in a range between $B = 50$ and 100 mT, the helical structure can be transformed to the ordered lattice of topologically protected vortex-like spin configurations, a magnetic skyrmion crystal (SkX) [8]. The typical characteristic length-scale of the skyrmion in B20 compounds ranges from a few tens to hundreds of nanometers, which corresponds to the small-angle scattering region for soft X-rays with energies matching the L absorption edges of transition metals [3].

A resonant soft X-ray scattering (RSXS) experiment was carried out at BL-16A. The setup was equipped with a high-vacuum chamber. The scattered intensity was collected by an in-vacuum charge coupled device (CCD) detector protected from the transmitted direct beam by a tungsten beamstop with a size of 0.2 – 0.3 mm situated at a fixed distance in front of the CCD matrix. A magnetic field produced by a Helmholtz coil up to 400 mT was applied parallel to the incident X-rays and perpendicular to the sample plane. A He-flow-type refrigerator was used to control the sample temperature.

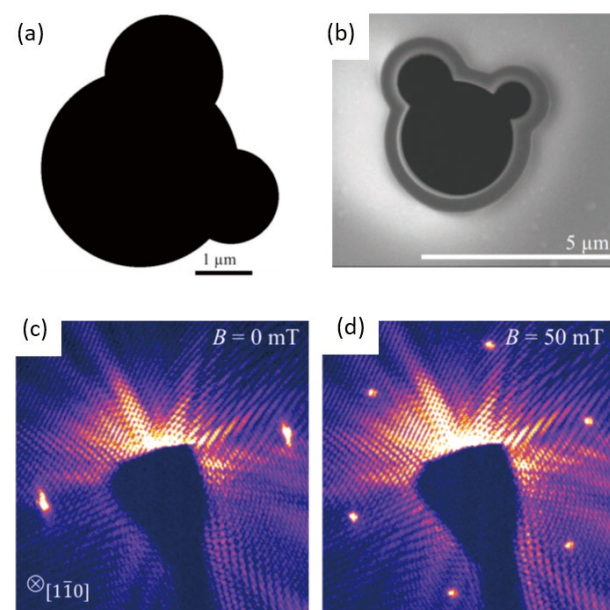


Figure 1: (a) A binary image used for real-space support in the iterative phase retrieval algorithm and (b) an SEM image of the sample aperture produced in the gold mask by FIB. Coherent resonant soft X-ray diffraction pattern from (c) helical magnetic structure and (d) magnetic skyrmion crystal.

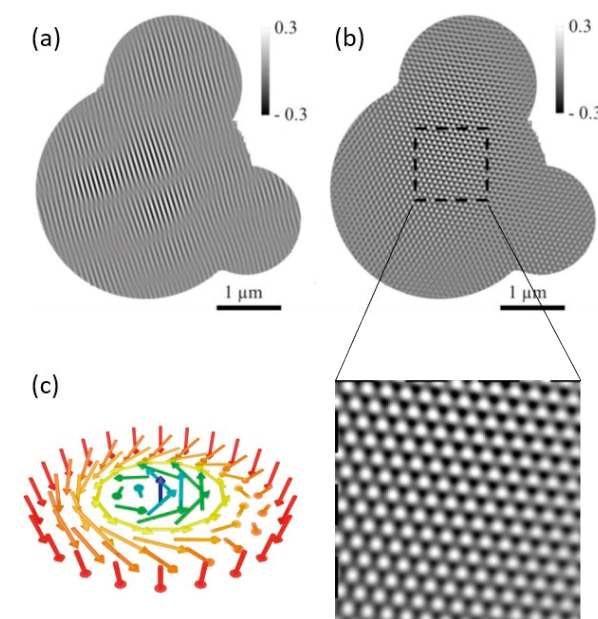


Figure 2: Imaginary part of the reconstruction of the magnetic texture of FeGe at (a) $B = 0$ mT (helical phase) and (b) $B = 50$ mT (SkX phase). The black rectangle in panel (b) indicates the magnification area shown in panel (c).

The experiment was performed with a single-crystalline thin plate of FeGe using soft X-rays at the resonant energy $E = 707$ eV corresponding to the L_3 absorption edge of Fe ion. Since the X-ray attenuation length for FeGe at this edge is a few hundreds of nanometers, a plate with a thickness of $l = 200$ nm was prepared by focused ion beam (FIB) milling and fixed to a Si_3N_4 membrane by a tungsten contact. The back side of the membrane was coated with a $4\text{-}\mu\text{m}$ Au absorbing layer to protect the detector from the transmitted X-ray beam. A binary image and an SEM image of the sample aperture produced in the gold mask by FIB are shown in Figs. 1(a) and (b), respectively. The asymmetric shape of the pinhole was chosen to provide better stagnation and verify the reliability of the phase retrieval algorithm. The aperture size was chosen based on the longitudinal coherence length (less than $10\ \mu\text{m}$) of the X-ray beam to satisfy the oversampling condition.

Small-angle scattering from a helical magnetic structure can be clearly observed at zero magnetic field [Fig. 1(c)] as two symmetric magnetic peaks corresponding to the single-domain helical state. When a magnetic field of $B = 50$ mT was applied, six magnetic peaks were clearly observed for the SkX state [Fig. 1(d)]. The resultant magnetic coherent X-ray diffraction patterns were employed for the phase retrieval. We used the hybrid-input-output (HIO) algorithm with improved noise tolerance and did not assume positivity or reality constraints. Reconstructed images obtained by 1000 individual runs of the algorithm with random initial phases were averaged. Imaginary parts of the reconstructed complex-valued images of the helical texture and skyrmion lattice shown in Figs. 2(a) and (b)

were obtained from RSXS patterns [Figs. 1(c) and 1(d)] measured at $B = 0$ mT and $B = 50$ mT, respectively. The black and white regions in these images indicate the magnetic components parallel and anti-parallel to the incident soft X-ray beams. Triangle skyrmion crystals are clearly reconstructed at $B = 50$ mT as shown in Fig. 2(c). The spatial resolution of the obtained magnetic structure is estimated to be a few tens of nanometers.

REFERENCES

- [1] J. Miao, T. Ishikawa, I. K. Robinson and M. M. Murnane, *Science* **348**, 530 (2015).
- [2] Y. Yamasaki, J. Fujioka, H. Nakao, J. Okamoto, T. Sudayama, Y. Murakami, M. Nakamura, M. Kawasaki, T. Arima and Y. Tokura, *J. Phys. Soc. Jpn.* **85**, 023704 (2016).
- [3] Y. Yamasaki, D. Morikawa, T. Honda, H. Nakao, Y. Murakami, N. Kanazawa, M. Kawasaki, T. Arima and Y. Tokura, *Phys. Rev. B* **92**, 220421 (2015).
- [4] Y. Okamura, Y. Yamasaki, D. Morikawa, T. Honda, V. Ukleev, H. Nakao, Y. Murakami, K. Shibata, F. Kagawa, S. Seki, T. Arima and Y. Tokura, *Phys. Rev. B*, **95**, 184411 (2017).
- [5] J. J. Turner, X. Huang, O. Krupin, K. A. Seu, D. Parks, S. Kevan, E. Lima, K. Kisslinger, I. McNulty, R. Gambino, S. Mangin, *Phys. Rev. Lett.*, **107**, 033904 (2011).
- [6] S. Eisebitt, J. Lüning, W. Schlotter, M. Lörger, O. Hellwig, W. Eberhardt, J. Stöhr, *Nature* **432**, 885 (2004).
- [7] V. Ukleev, Y. Yamasaki, D. Morikawa, N. Kanazawa, Y. Okamura, H. Nakao, Y. Tokura, T. -H. Arima, *QUANTUM BEAM SCIENCE* **2**, [1] 3-1 (2018).
- [8] X. Z. Yu, N. Kanazawa, Y. Onose, K. Kimoto, W. Z. Zhang, S. Ishiwata, Y. Matsui and Y. Tokura, *Nat. Mater.* **10**, 106 (2011).

BEAMLIN

BL-16A

Y. Yamasaki (¹NIMS, ²JST-PRESTO, ³RIKEN)